An improvement on the modelling of non-transferred plasma torches



2000 J. Phys. D: Appl. Phys. 33 134

(http://iopscience.iop.org/0022-3727/33/2/307)

J. Phys. D: Appl. Phys. **33** (2000) 134–140. Printed in the UK PII: S0022-3727(00)06228-8

# An improvement on the modelling of non-transferred plasma torches

**R C Bianchini†, R C Favalli‡, M M Pimenta§ and R N Szente†‖**

† Departamento de Física Aplicada, Instituto de Física, Universidade de São Paulo, Cidade Universitária, São Paulo, cep 05315-900, Brazil
‡ Divisão de Materiais, Instituto de Pesquisas Energéticas e Nucleares, Universidade de São Paulo, Cidade Universitária, São Paulo, cep 05315-900, Brazil
§ Departamento de Engenharia Mecânica, Escola Politécnica, Universidade de São Paulo, Cidade Universitária, São Paulo, cep 05315-900, Brazil

E-mail: szente@ipt.br

Received 21 July 1999, in final form 22 October 1999

**Abstract.** In the modelling of non-transferred plasma torches, the electrical potential is normally used in the same way as in the simulation of transferred plasma torches. This approach results in physically questionable current density profiles. A modification is proposed in the manner that the electrical potential is used in the simulation of non-transferred plasma torches. The new model provides in physically acceptable results. A comparison of the results obtained from the two models (the previously used and the presently proposed), shows differences of up to 50% in the velocity and 20% in the temperature were found. Tests were performed with the new model showing the possibility of using it for a broad range of parameters.

## 1. Introduction

Thermal plasmas were first used industrially in the early 1950s; interest in plasmas has grown in the last ten years. Typical applications of this technology include materials processing (spraying, production of ceramic parts, synthesis of compounds such as titanium dioxide, silicon carbide, silicon nitride, superconductors) and metallurgy (blast furnaces, production of special steel and ferro-alloys, cutting, recovery of metal fines). In the last five years, thermal plasmas have been extensively employed to treat residues or remediate environmental problems such as: hospital waste, destruction of toxic materials, vitrification of asbestos, remelting of incineration ashes, treatment of galvanic sludges, mercury contaminated soils and many others [1–3].

It is very common that the development of plasma torches, specifically for certain applications, is conducted empirically, implying high costs and long development times for the equipment construction, modifications and tests. An important auxiliary tool in the development of a torch can be the simulation of the plasma jet flow using mathematical models and numerical schemes. This approach not only reduces the time spent for developing a plasma torch, but also helps the understanding of the basic physical phenomena involved in the torch operation, both in the plasma flow and in the electric arc region, where measurements are extremely complex.

The first modelling articles published concerning non-transferred arcs dealt with the simulation of the plasma jet only, without calculating the electrical potential [4–7]. The disadvantage of such an approach is the necessity of specifying the velocity and temperature profiles of the torch nozzle exit and to calculate from there the plasma jet profiles.

In the last few years, the modelling of non-transferred plasma torches has been improved by Kovitya *et al* [8] who adapted the original model proposed by Hsu *et al* [9] for the simulation of the electrical potential and current densities of a transferred arc. This more recent approach allows the inclusion of the arc region in the calculations, therefore eliminating the shortcoming of the previous modelling, i.e. the values of temperature and velocity calculated inside the torch were used as boundary conditions at the torch nozzle exit. The model involving the electrical potential and current densities has been used by several authors [10–13].

However, when the above described model was used, some results which were physically difficult to explain were obtained by the present authors, including the presence of high values of electrical potential at different locations along the gap between the electrodes (‘bumps’). It was felt that a more systematic study was needed in order to investigate those unexpected behaviours; the present study is an attempt in that direction.

The main objectives of the present study are: (i) to present the physical shortcomings of the previous model used to simulate non-transferred plasma torches; (ii) to suggest modifications in order to improve the previous model; (iii) to compare the results of both approaches; (iv) to conduct preliminary tests for the proposed model.

The theory involved in the modelling of plasma torches is presented in section 2. Section 3 introduces the improvement

‖ Author to whom correspondence should be addressed

0022-3727/00/020134+07$30.00 

of the model of non-transferred plasma torches and compares the results obtained by the two models. A short parametric study to test the developed computer program is shown in section 4. The main conclusions reached in this study are presented in section 5.

## 2. Theory

Physical modelling of plasma torches is commonly conducted under some simplifying assumptions, also adopted here, such as: (i) the plasma is optically thin; (ii) the arc is in local thermodynamic equilibrium (LTE); (iii) heat dissipation due to viscosity and gravity effects are negligible; (iv) the plasma flow is assumed to be steady and rotationally symmetric; (v) there is no swirl. Turbulence effects are not included in this paper and are the subject of a future article.

The plasma flow is generally modelled using the conservation of mass, momentum and energy equations given below.

(i) Mass

$$\frac{1}{r}\frac{\partial}{\partial r}(r\rho v) + \frac{\partial}{\partial z}(\rho u) = 0. \tag{1}$$

(ii) Radial momentum

$$\frac{1}{r}\frac{\partial}{\partial r}(r\rho v^2) + \frac{\partial}{\partial z}(\rho u v) = \frac{1}{r}\frac{\partial}{\partial r}\left(2r\mu\frac{\partial v}{\partial r}\right) + \frac{\partial}{\partial z}\left[\mu\left(\frac{\partial u}{\partial r} + \frac{\partial v}{\partial z}\right)\right] - 2\mu\frac{v}{r^2} - \frac{\partial p}{\partial r} - j_z B_\theta. \tag{2}$$

(iii) Axial momentum

$$\frac{1}{r}\frac{\partial}{\partial r}(r\rho u v) + \frac{\partial}{\partial z}(\rho u^2) = \frac{1}{r}\frac{\partial}{\partial r}\left[r\mu\left(\frac{\partial u}{\partial r} + \frac{\partial v}{\partial z}\right)\right] + \frac{\partial}{\partial z}\left(2\mu\frac{\partial u}{\partial z}\right) - \frac{\partial p}{\partial z} + j_r B_\theta. \tag{3}$$

(iv) Energy

$$\frac{1}{r}\frac{\partial}{\partial r}(r\rho v h) + \frac{\partial}{\partial z}(\rho u h) = \frac{1}{r}\frac{\partial}{\partial r}\left(r\frac{k}{C_p}\frac{\partial h}{\partial r}\right) + \frac{\partial}{\partial z}\left(\frac{k}{C_p}\frac{\partial h}{\partial z}\right) + \frac{j_r^2 + j_z^2}{\sigma} - S_r \tag{4}$$

where $u$ and $v$ are the axial and radial velocity components, $\rho$ is the mass density, $z$ and $r$ are the coordinates in the axial and radial directions, $p$ is the pressure, $h$ is the specific enthalpy, $C_p$ is the specific heat at constant pressure, $k$ and $\sigma$ are the thermal and electrical conductivities, respectively; $j_r$ and $j_z$ are the radial and axial current densities, $B_\theta$ is the azimuthal component of the magnetic field and $S_r$ is the radiation heat loss.

To include the arc region in the simulation, the conservation of the electrical current must be added to this set of governing equations

$$\frac{1}{r}\frac{\partial}{\partial r}\left(r\sigma\frac{\partial \Phi}{\partial r}\right) + \frac{\partial}{\partial z}\left(\sigma\frac{\partial \Phi}{\partial z}\right) = 0 \tag{5}$$

where $\Phi$ is the electrical potential.

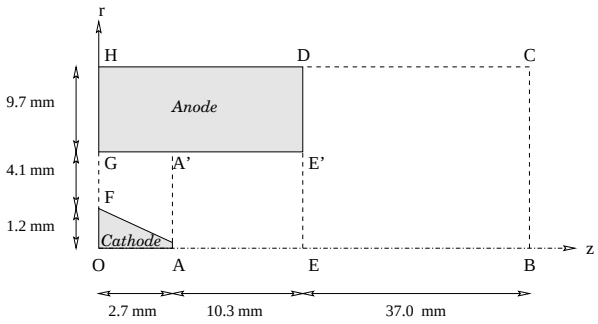


**Figure 1.** Computational domain of the plasma torch.

The current densities and the azimuthal magnetic field used as source terms in the equations of momentum and energy are obtained from the following expressions:

$$j_z = -\sigma\frac{\partial \Phi}{\partial z} \qquad j_r = -\sigma\frac{\partial \Phi}{\partial r} \tag{6}$$

$$\frac{1}{r}\frac{\partial}{\partial r}(r B_\theta) = \mu_0 j_z \tag{7}$$

where $\mu_0$ is the permeability of the free space. The thermodynamic and transport properties for argon were taken from the literature [14, 15].

## 3. Modelling of non-transferred plasma torch

The computational domain and boundary conditions used to solve the set of governing equations are presented in section 3.1. In sections 3.2 and 3.3 are preserved the results obtained by models one and two (the previously used and the one presented here, respectively); comparisons between the models are given in section 4.1.

### 3.1. Computational domain and boundary conditions

A computer program was developed to solve the set of governing equations presented above for a non-transferred plasma torch. The computational domain used to establish the boundary conditions for all dependent variables is presented in figure 1.

The axial velocity ($u$) at the entrance of the torch is determined by specifying the gas flow rate. The radial velocity ($v$) is zero there. No-slip conditions are assumed on the electrodes surfaces, i.e. $u = v = 0$. On the centre line AB, $\partial u/\partial r = v = 0$. Free-boundary conditions for BC and CD are assumed, i.e. $\partial(\rho u)/\partial z = \partial v/\partial z = 0$ and $u = \partial(r\rho v)/\partial r = 0$, respectively.

The boundary conditions for the enthalpy are given in terms of temperature and then converted into the enthalpy of the respective gas. The temperatures at the entrance of the torch and at CD surface are assumed to be equal to 500 K. The surfaces of the cathode and of the anode are assumed to be at 3000 K and 1000 K, respectively. On the centre line $\partial h/\partial r = 0$, and at BC $\partial h/\partial z = 0$.

The boundary conditions for the electrical potential $\Phi$ are set on the surface AA′EE′. On line AA′, the electrical

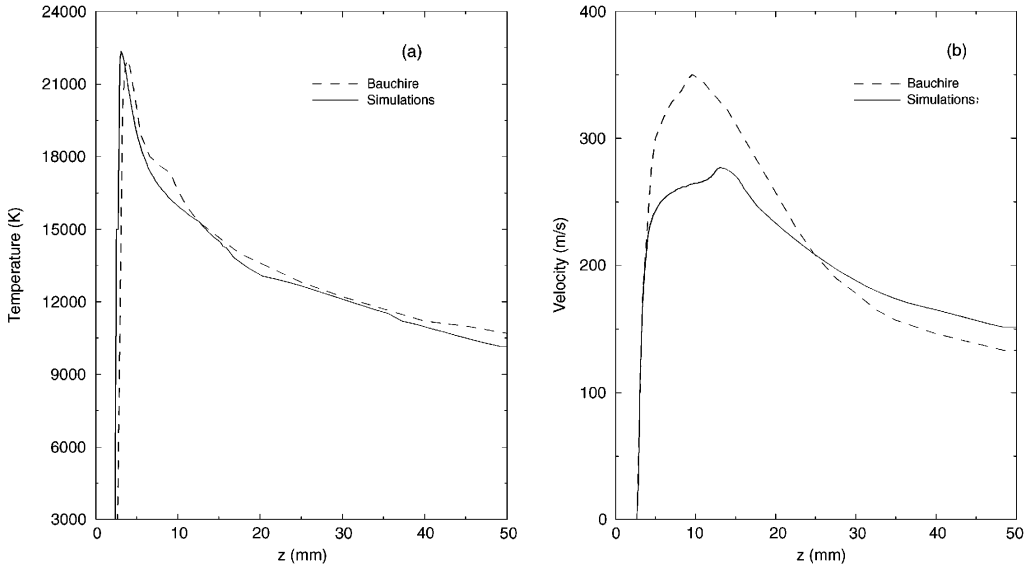


**Figure 2.** (a) Temperature and (b) velocity profiles at the centre line generated here (full curve) and obtained by Bauchire *et al* (broken curve). The gas flow rate was 60 l min$^{-1}$ and the current was 200 A.

potential is determined by specifying a radial current density profile for $j_z$, the axial component of current density:

$$j_z(r) = j_0 \, \mathrm{e}^{-r/r_c} \tag{8}$$

where $j_0$ and $r_c$ are constants which depend on the current. On line AB, $\partial j_z/\partial r = j_r = 0$; $j_z = j_r = 0$ in ED and $\Phi = 0$ at the anode. The potential at the cathode is taken to be positive with respect to the anode. In reality this is exactly the opposite to that observed experimentally. In the modelling of plasma torches, the fact that the cathode is the positive electrode is not important, as long as the difference between the potentials of the electrodes has the right value.

For simplicity, we refer to the model used previously [8–13] as model one and the modified model suggested here is called model two. Model one assumes that equation (8) is valid along the whole line AA′ while model two uses that equation just near the cathode, combining linear and parabolic profiles for the remaining boundary. In the following, the obtained results with both models are shown, compared and discussed.

### 3.2. Model one

A computer code was developed to simulate the plasma flow inside and outside of a non-transferred plasma torch using the model described in section 2. The obtained results corroborate well those of Bauchire *et al* [13], using similar geometry and operating conditions, as can be seen in figure 2. The 0 in the $z$ and $r$ directions corresponds to the point O of computational domain sketched in figure 1.

The differences observed in the results shown above are probably due to the set of parameters chosen in each work, including differences in the geometry of the torch (particularly the smaller anode adopted by Bauchire *et al* [13] than that used here), boundary conditions and initial values of temperature and velocity. It could also be partially due to possible differences in the values of $j_0$ and $r_c$, which

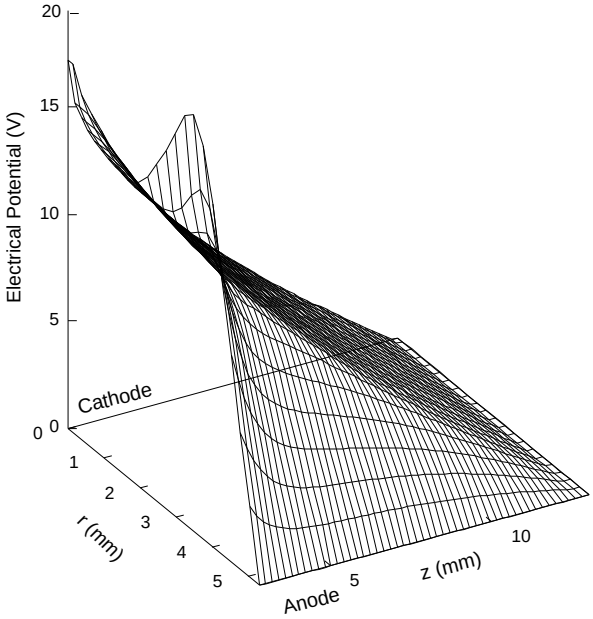


**Figure 3.** Electrical potential calculated using model one for 40 l min$^{-1}$ and 100 A.

were not specified in the reference. The maximum difference between the two results for axial velocity, which is always the most sensitive parameter, is 25% at an axial distance of approximately 13 mm, decreasing to 10% at the end of the computational domain. For temperature, differences are smaller than 5%.

However, the use of equation (8) over the entire surface AA′ to calculate the boundary condition for the electrical potential results in a 'bump' on its profile when using the geometry and boundary conditions adopted here, as can be seen in figure 3. As the plasma gas is injected axially into the plasma torch, the region located in the middle of the gap between the electrodes will be at considerably lower temperature than the

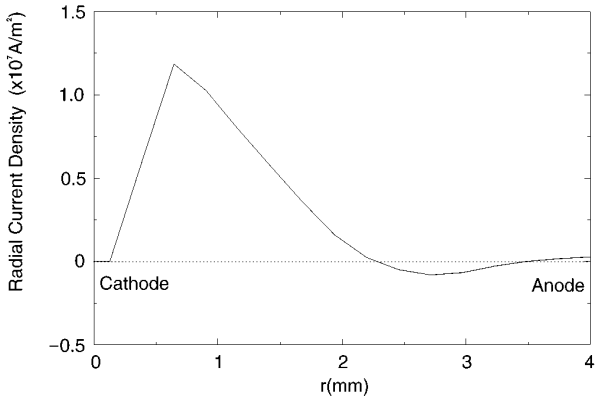


**Figure 4.** Radial current density calculated at AA′ using model one for 40 l min$^{-1}$ and 100 A.

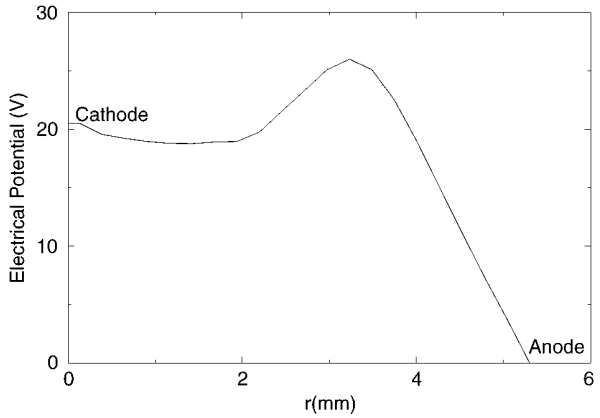


**Figure 5.** Electrical potential calculated at line AA′ using model one for 100 l min$^{-1}$ and 100 A.

region closer to the cathode. Consequently, the electrical conductivity, which decreases with temperature, will have lower values in the midway region between the electrodes, even when using a modified expression for calculating the electrical conductivity for temperatures below 8000 K as proposed by others researchers [8, 10]. The low values of the electrical conductivity result in a bump on the electrical potential profile, as correctly predicted by the computer code, but not verified experimentally.

A cooling of the central region where the arc is located would result experimentally in a increase of the overall voltage of the arc, cause by either or a combination of two factors: an increase of the arc length (the arc bends and seeks regions of higher temperatures—higher electrical conductivity) or a decrease in the electrical conductivity. This increase in the overall arc voltage is commonly observed experimentally for that situation (cooling of the arc); however, no 'local' increase of the arc voltage, as for instance, in the middle of the arc region, was ever observed.

The present mathematical and physical modelling of the arc region and the plasma torch cannot consider an increase of the overall voltage if the central region of the arc is cooled; the computer code calculates correctly the increase of the arc voltage 'locally' but this information cannot be transmitted 'backwards' to the cathode region (where the arc voltage is supposed to have its higher value—considering here the

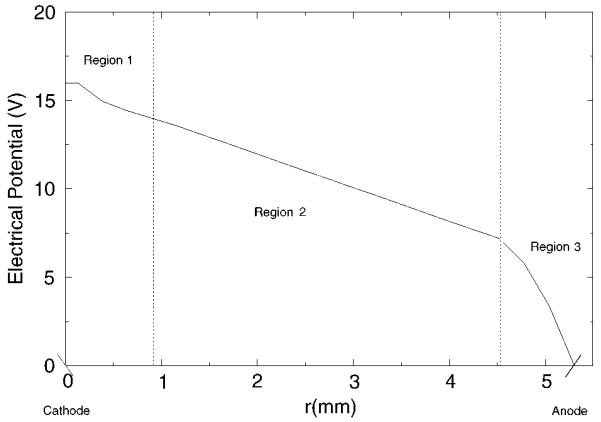


**Figure 6.** Regions for the boundary conditions of the electrical potential on the line AA′.

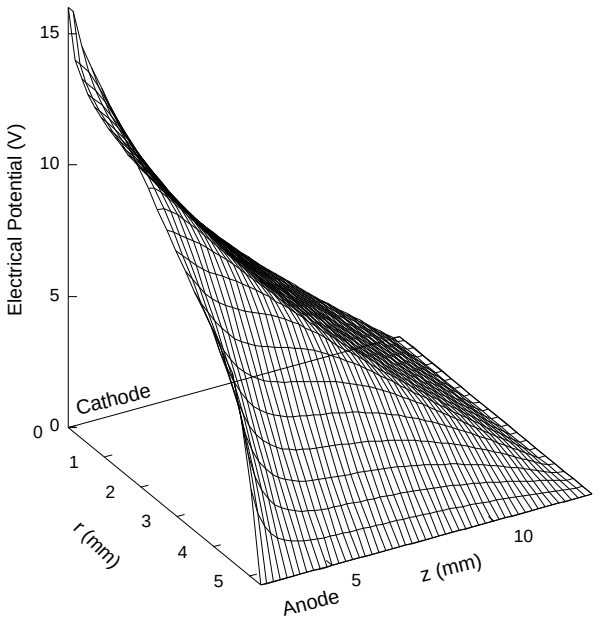


**Figure 7.** Electrical potential calculated using model two for 40 l min$^{-1}$ and 100 A.

characteristics of the modelling presented before of a positive voltage for the cathode and zero potential for the anode) and therefore no overall voltage increase of the arc voltage can be obtained in the calculations.

If different torch geometries or operating conditions are used (for instance if the plasma gas is injected in a region far from where the arc is located or if swirl is considered, resulting in a flatter velocity and temperature distribution profile of the plasma gas at the arc region), the bump of the electrical potential mentioned above would decrease considerably, even disappearing in some conditions. Since the radial current density in this model is calculated as a derivative of the electrical potential in the $r$ direction (see equation (6)), an inversion of the sign of the current density occurs, i.e. there is an electron counterflow. Figure 4 shows $j_r$ along the radial distance.

Inversions on the current density sign are not acceptable since experimentally it would imply a large change of the arc behaviour, which has never been measured or reported.

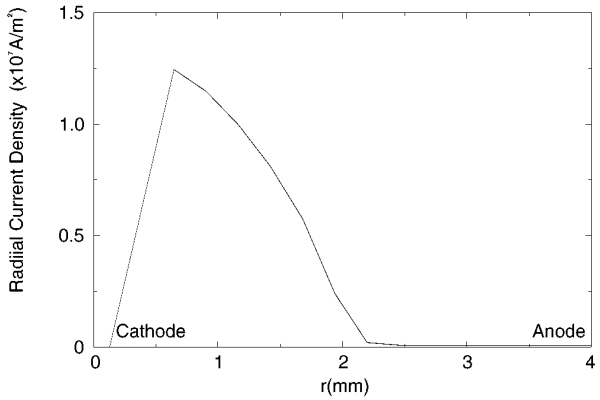


**Figure 8.** Radial current density calculated at line AA′ using model two for 40 l min$^{-1}$ and 100 A.

As the gas flow rate is increased from 40 to 100 l min$^{-1}$, the 'bump' increases due a higher cooling of the arc, resulting in an even smaller electrical conductivity. The maximum value of the electrical potential is reached midway between the electrodes, as shown in figure 5, and not at the cathode tip. These results indicate that no arc could exist before the maximum value of the electrical potential (in the region around the centre of the gap between the two electrodes), which is not the fact.

This shortcoming could be possibly avoided if simulations of the non-transferred plasma torches were conducted in three dimensions. In this situation, the condition of axial symmetry is no longer required, allowing therefore the exact localization of the electric arc and avoiding some of the problems indicated above. But three-dimensional modelling of non-transferred torches is still a difficult task; a much more complex program is needed as well as considerably more computational processing time and memory. A possible methodology to improve the two-dimensional modelling of non-transferred plasma torches is shown in the next section.

### 3.3. Model two

A possible solution for the problems presented above is to consider the boundary condition based on the axial current density of equation (8) just in a region near the cathode ($\approx$1 mm or less), assuming from there on a linear and a parabolic profile for the electrical potential, respectively. It should be noted here that the values of the electrical potential (close to the cathode) are obtained directly from the simulations and not imposed as boundary conditions. Only the form that the electrical potential should have is stipulated (linear and parabolic). The assumption for the form of the electrical potential has two justifications: (i) the only experimentally measured current density is at the cathode surface [9]. Therefore close to the cathode, the assumed current density profile is more accurate as well as the value of the electrical potential; (ii) a linear and a parabolic profile coupled with that given by equation (8) close to the cathode result in an electrical potential profile similar to that suggested in the literature and based on experimental and theoretical analysis [14]. Other electrical potential profiles can be

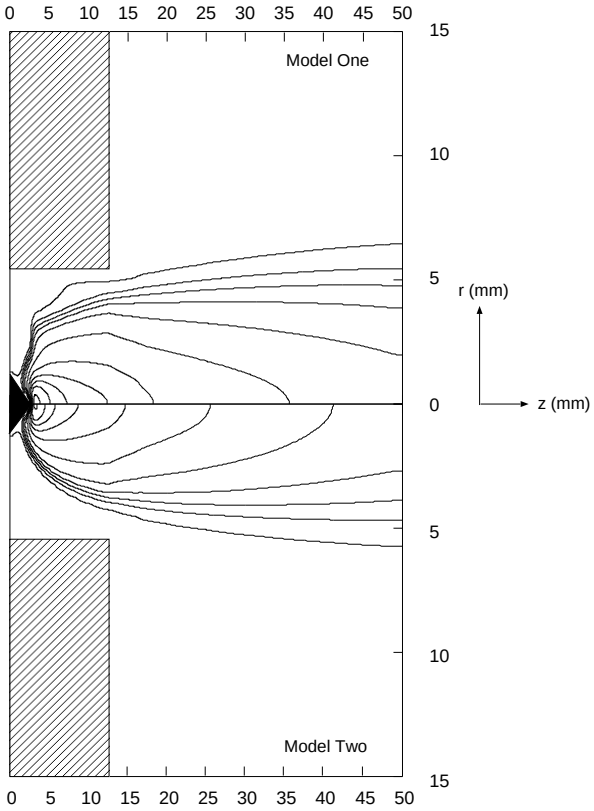


**Figure 9.** Isotherms generated using model one and two for 40 l min$^{-1}$ and 100 A. Outermost line is 2000 K and the contour steps are 2000 K.

used as long as they have physical meaning and provide acceptable current density and electrical potential profiles. Figure 6 shows the form proposed here for the electrical potential.

In region 1 the radial equation for the axial current density is assumed valid, (see equation (8) for the boundary condition). The electrical potential is then calculated in this region. In region 2, a linear profile for the electrical potential is fitted from the last grid point of region 1 until approximately 0.8 mm before the anode; for 100 A of current and 40 l min$^{-1}$ of gas flow rate, the linear profile has an angular coefficient of $-1.9014 \times 10^3$ and a linear coefficient of 15.77. In the last region, region 3, a parabolic curve is fitted from the last grid point of the linear region (which is chosen as the vertex) until the anode (zero electrical potential). The formula used to describe the parabolic profile in this case is given by $y = a_1 + a_2(x - b_1) + a_3(x - b_1)(x - b_2)$ where, for 100 A and 440 l min$^{-1}$, $a_1 = 0$, $a_2 = 7.4051 \times 10^3$, $b_1 = 3.2327$, $a_3 = -7.15828133 \times 10^6$ and $b_2 = 4.267$.

In this new approach, (model two), the boundary conditions for the temperature and velocity are the same as those described previously, as well as the computational domain.

In figure 7 is shown the electrical potential in region AA′EE′ which results from the approach just described.

The radial current density now shows an acceptable profile without sign changes, as shown in figure 8.

It has been verified that the approach described above can be used for distances as small as 0.4 mm from the cathode

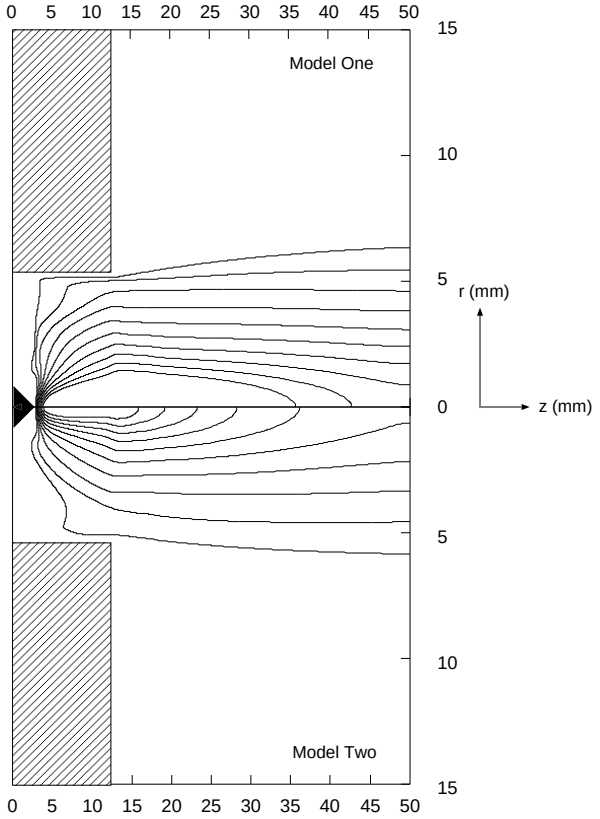


**Figure 10.** Lines of constant velocities generated using models one and two for 40 l $min^{-1}$ and 100 A. The outermost line is 40 m $s^{-1}$ and the contour steps are 20 m $s^{-1}$.

and, in this case, the boundary conditions for the current density are given by equation (8) up to 0.4 mm, followed by linear and parabolic electrical potential profiles. It should be pointed out that both models do not take the electrode fall into account.

## 4. Results and discussion

Some results obtained using models one and two are presented and discussed below, followed by a short parametric study using model two.

### 4.1. Comparison between models one and two

The electrical potential and radial current density calculated using both model one and two are presented in figures 3, 4, 7 and 8. The operating conditions are: gas flow rate of 40 l $min^{-1}$ and an arc current of 100 A. The same geometry and boundary conditions as previously described were used for both models.

The temperature and velocity profiles for both models one and two were compared and are shown in figures 9 and 10. In the central region of the plasma jet, the temperature generated in model one presents values 20% greater than that presented by model two; for the velocity, the differences reach 50%, as can be seen below.

Therefore using model two not only provides physically acceptable results but also generates temperature and velocity profiles considerably different from those obtained with

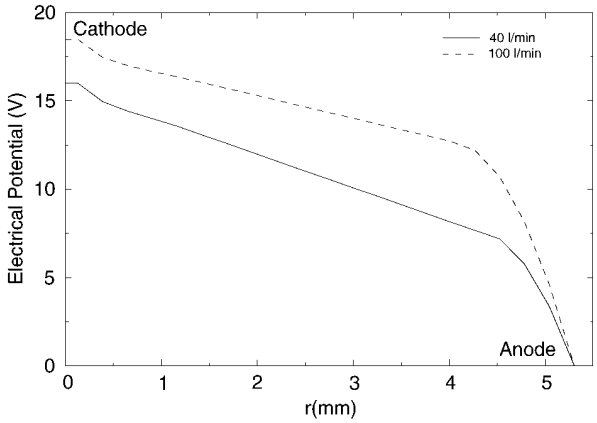


**Figure 11.** Electrical potential calculated for flow rates of 40 and 100 l $min^{-1}$.

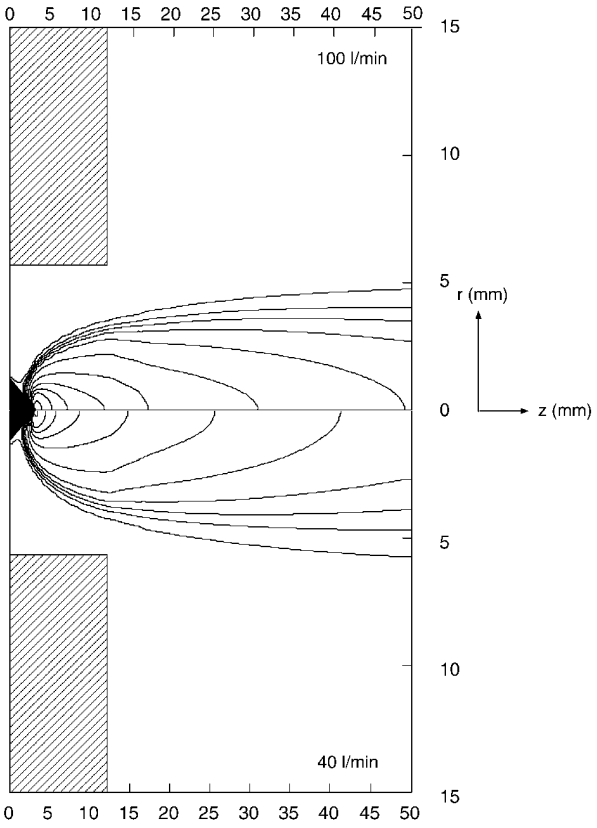


**Figure 12.** Isotherms generated for flow rates of 40 and 100 l $min^{-1}$. The outermost line is 2000 K and the contour steps are 2000 K.

model one. This fact could have an important impact on the modelling of non-transferred plasma torches; at the moment, a comparison between the results from the modelling and experiments are being conducted and will be the subject of a future article.

### 4.2. Parametric test

The gas flow rate was varied in order to verify the validity of the developed computer code. The results obtained in those simulations, using model two, are presented next.

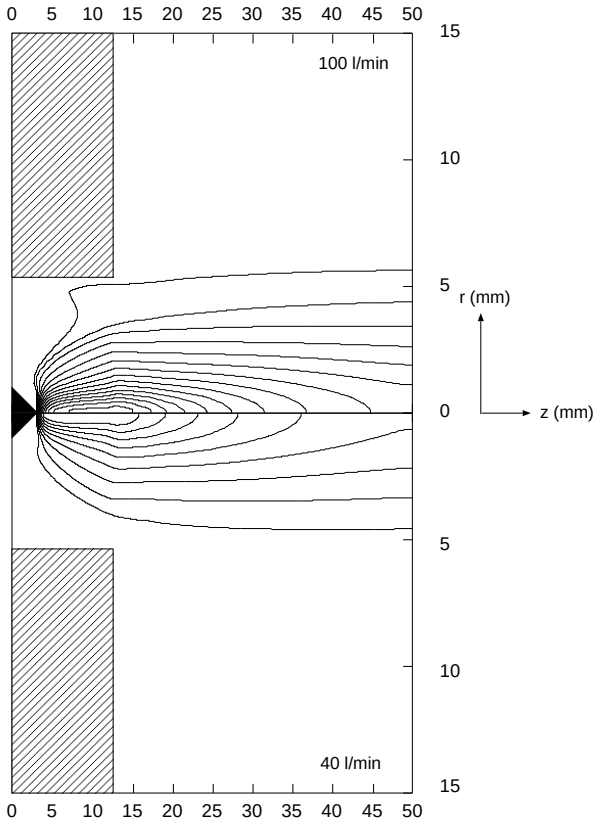


**Figure 13.** Lines of constant velocities generated for flow rates of 40 and 100 l min$^{-1}$. The outermost line is 40 m s$^{-1}$ and the contour steps are 20 m s$^{-1}$.

**4.2.1. Gas flow rate.** The effect of the gas flow rate on the electrical potential, temperature and velocity profiles were studied and the results obtained are shown in figures 11, 12 and 13, respectively. It can be seen that the electrical potential rises when the gas flow rate is increased from 40 to 100 l min$^{-1}$ as expected and observed experimentally, since more energy is needed for ionizing and heating the gas.

Due mainly to the increase of the electrical potential, the temperature and velocity profiles also changes for higher gas flow rates; the plasma jet temperature profile for a gas flow rate of 100 l min$^{-1}$ becomes approximately 15% larger than that calculated for 40 l min$^{-1}$.

The velocity profile presents a similar behaviour as that of the temperature, with values 44% higher for higher flow rates.

## 5. Conclusion

In this article it has been shown that the modelling of non-transferred plasma torches, based on the approach used for transferred ones can lead to inconsistent results for the current density and electrical potential. It was found that the use of a single equation for the boundary condition of the electrical potential can lead to physically unreasonable results for the modelling of non-transferred plasma torches. A modification of the model previously used has been proposed here, consisting of using the radial profile of the axial current density only in the region near the cathode tip and establishing, from there on, two profiles for the electrical potential: a linear one and a parabolic one, respectively. No values for the electrical potential were imposed, only the form (linear and parabolic); the total current was maintained in the same was as that specified for the calculation. The suggested modifications resulted in consistent and physically acceptable radial current density and electrical potential profiles. Comparison between the two models shows differences of around 20% for the temperature and 50% for the velocities of the plasma jet, using the same geometry and boundary conditions. The proposed model was shown to simulate non-transferred plasma torches for different gas flow rates, generating consistent temperature and velocity profiles. The simulations show that the differences between the two models tend to rise together with the other parameters, e.g. the gas flow rate is increased.

## Acknowledgments

Financial support from FAPESP through scholarships for RCB, process number 97/06148-5, and RCF, process number 96/11957-7, are gratefully acknowledged.

## References

[1] Szekely J and Apelian D 1987 *Plasma Process in Synthesis of Materials* (Anaheim: MRS)
[2] EPRI Workshop 1987 *Research Opportunities for Plasma Processing* (Palo Alto: EPRI Centre for Materials Protection)
[3] Szente R N 1995 *Industrial Applications of Thermal Plasmas* vol 345 (Paraná, Br: AIP) p 487
[4] Mazza A 1983 Studies of an arc plasma reaction for thermal plasmas synthesis *PhD Thesis* Mechanical Engineering, University of Minnesota
[5] Lee Y C 1984 Modelling work in thermal plasma processing *PhD Thesis* Mechanical Engineering, University of Minnesota
[6] Dilawari A H, Szekely J, Batdorf J, Detering R and Shaw C B 1990 The temperature profiles in an argon plasma issuing into an argon atmosphere: a comparison of measurements and predictions *Plasma Chem. Plasma Process.* **10** 321
[7] Ramshaw J D and Chang C H 1992 Computational fluid dynamics modeling of multicomponent thermal plasmas *Plasma Chem. Plasma Process.* **12** 299
[8] Kovitya P, Scott D A and Haddad G N 1988 Two dimensional modeling of plasma torches (CSIRO Division of Applied Physics) *Technical Report*
[9] Hsu K C, Etemadi K and Pfender E 1983 Study of the free-burning high-intensity argon arc *J. Appl. Phys.* **54** 1293
[10] Scott D A, Kovitya P and Haddad G N 1989 Temperature in the plume of a d.c. plasma torch *J. Appl. Phys.* **66** 5232
[11] Murphy A B and Kovitya P 1993 Mathematical model and laser-scattering temperature measurements of a direct-current plasma torch discharging into air *J. Appl. Phys.* **73** 4759
[12] Paik S, Huang P C, Heberlein and Pfender E 1993 Determination of arc root position in a d.c. plasma torch *Plasma Chem. Plasma Process.* **13** 379
[13] Bauchire J M, Gonzalez J J and Gleizes A 1997 Modelling of a d.c. plasma torch in laminar and turbulent flow *Plasma Chem. Plasma Process.* **17** 409
[14] Boulos M I, Fauchais P and Pfender E 1994 *Thermal Plasmas—Fundamentals and Applications* vol 1 (New York: Plenum) p 10
[15] Paik S, Hawkes G and Nguyen H D 1995 Effect of working gases on thermal plasma waste treatment *Plasma Chem. Plasma Process.* **15** 677